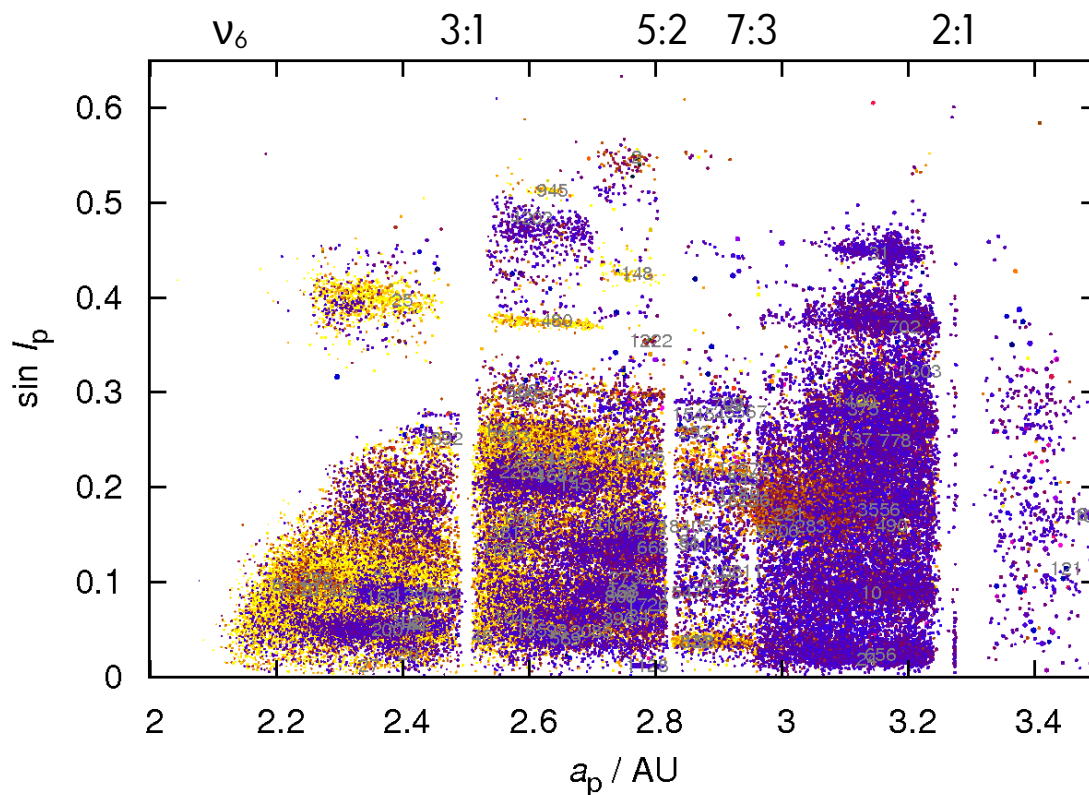


Simulations of asteroid families: knowns and unknowns

Miroslav Brož¹

¹ Charles University in Prague, Czech Republic



Milani & Knežević (2003)
Masiero et al. (2011)

Outline

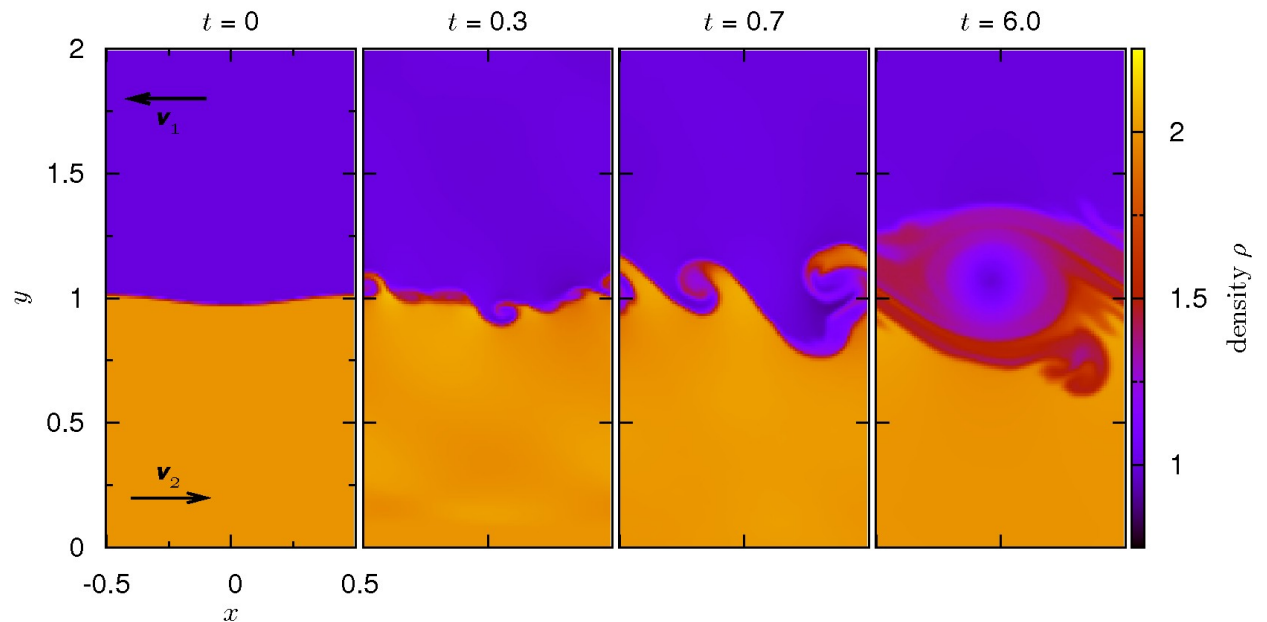
of the talk

1. general problems
2. methods
3. uncertainties & systematics
4. applications
5. future applications

serious

Five problems

- turbulence
- chaos
- irreversibility
- stochasticity
- $t = 0$



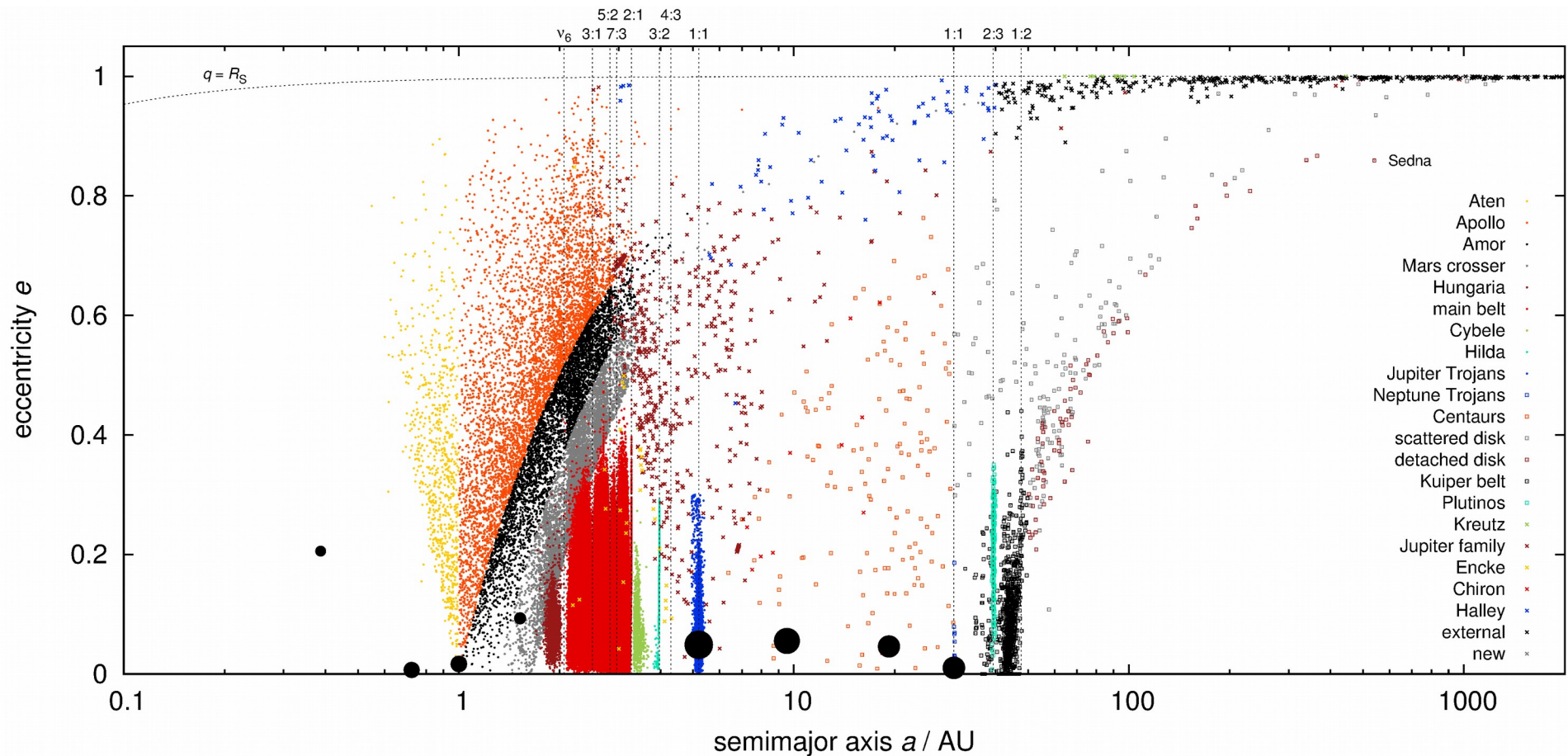
Kelvin-Helmholtz instability
Pluto code (Mignone et al. 2007)

additional instabilities:
Rayleigh-Taylor
magneto-rotational (Flock et al. 2013)
streaming (Johansen et al. 2007)

↓
an **inverse** problem
(except young families)

Observations ← usually taken @ 4.56 Gyr

- orbital distribution → families: MB, Hildas, Trojans of J & M, TNOs, irregular moons, ...



Types of numerical **Methods**

- hydrodynamic (e.g. SPH by Benz & Asphaug 1999)
 - N -body (Levison & Duncan 1994)
 - Monte-Carlo (Morbidelli et al. 2009)
 - initial conditions
 - boundary conditions
 - (material) parameters
 - parametric relations ← too complicated physics
 - (formal) uncertainties
 - systematics (!)
- lagrangian
vs eulerian

N -body **Swift integrator**

We use a symplectic integration scheme (Levison and Duncan 1994), denoted as kick–drift–kick, where the ‘kick’ (actually, a perturbation) is performed as:

$$\dot{\mathbf{r}}_{n+1} = \dot{\mathbf{r}}_n + \ddot{\mathbf{r}} \frac{\Delta t}{2}, \quad (3)$$

and the ‘drift’ corresponds to an analytical solution of the two-body problem (the Sun–asteroid), which involves a numerical solution of the transcendent Kepler equation:

$$M = E - e \sin E, \quad (4)$$

$$\mathbf{r}_{n+1} = p(E)\mathbf{r}_n + q(E)\dot{\mathbf{r}}_n, \quad (5)$$

$$\dot{\mathbf{r}}_{n+1} = \dot{p}(E)\mathbf{r}_n + \dot{q}(E)\dot{\mathbf{r}}_n; \quad (6)$$

we account for gravitational perturbations by planets, expressed in the heliocentric frame:

$$\ddot{\mathbf{r}}_j = \sum_i \left[-\frac{Gm_i}{r_i^3} \mathbf{r}_i - \frac{Gm_i}{r_{ji}^3} \mathbf{r}_{ji} \right], \quad (7)$$

possibly, the planetary migration, in an analytical way (Malhotra 1995), and also eccentricity damping (Morbidelli et al. 2010):

$$\dot{\mathbf{r}}_{n+1} = \dot{\mathbf{r}}_n \left[1 + \frac{\Delta v}{\dot{r}} \frac{\Delta t}{\tau_{\text{mig}}} \exp\left(-\frac{t - t_0}{\tau_{\text{mig}}}\right) \right], \quad (8)$$

Swift integrator (cont.)

as of Brož et al. (2011)

the Yarkovsky thermal effect (Vokrouhlický 1998, Vokrouhlický and Farinella 1999):

$$f_X(\zeta) + if_Y(\zeta) = -\frac{8}{3\sqrt{3}\pi} \Phi t'_{1-1}(R'; \zeta), \quad (9)$$

$$f_Z(\zeta) = -\frac{4}{3} \sqrt{\frac{2}{3\pi}} \Phi t'_{10}(R'; \zeta), \quad (10)$$

$$\Phi \equiv \frac{(1-A)\mathcal{E}_*\pi R^2}{m_j c_{\text{vac}}}, \quad (11)$$

the YORP effect (Čapek and Vokrouhlický 2004):

$$\dot{\omega} = cf_k(\gamma), \quad (12)$$

$$\dot{\gamma} = \frac{cg_k(\gamma)}{\omega}, \quad (13)$$

$$c \equiv c_{\text{YORP}} \left(\frac{a}{a_0}\right)^{-2} \left(\frac{R}{R_0}\right)^{-2} \left(\frac{\rho}{\rho_0}\right)^{-1}, \quad (14)$$

mass shedding beyond the critical angular frequency (Pravec and Harris 2000):

$$\omega_{\text{crit}} = \sqrt{\frac{4}{3}\pi G\rho}, \quad (15)$$

and random collisional reorientations with the time scale (Farinella et al. 1998):

$$\tau_{\text{reor}} = B \left(\frac{\omega}{\omega_0}\right)^{\beta_1} \left(\frac{R}{R_0}\right)^{\beta_2}. \quad (16)$$

Boulder code

(Morbidelli et al. 2009)

- Monte-Carlo approach
- number of disruptions
- parametric relations (SPH)
- largest remnant
- largest fragment
- SFD slope of fragments
- dynamical decay

pseudo-random-number generator
for rare collisions within one time step

specific energy $Q = \frac{1}{2} m_i v^2 / M_{\text{tot}}$

Q_D^* ... scaling law

focussing

$$n_{ij} = p_i(t) f_g \frac{(D_i + d_j)^2}{4} n_i n_j \Delta t$$

$$M_{\text{LR}} = \left[-\frac{1}{2} \left(\frac{Q}{Q_D^*} - 1 \right) + \frac{1}{2} \right] M_{\text{tot}} \quad \text{for } Q < Q_D^*$$

$$M_{\text{LR}} = \left[-0.35 \left(\frac{Q}{Q_D^*} - 1 \right) + \frac{1}{2} \right] M_{\text{tot}} \quad \text{for } Q > Q_D^*$$

$$M_{\text{LF}} = 8 \times 10^{-3} \left[\frac{Q}{Q_D^*} \exp \left(- \left(\frac{Q}{4Q_D^*} \right)^2 \right) \right] M_{\text{tot}}$$

$$q = -10 + 7 \left(\frac{Q}{Q_D^*} \right)^{0.4} \exp \left(- \frac{Q}{7Q_D^*} \right)$$

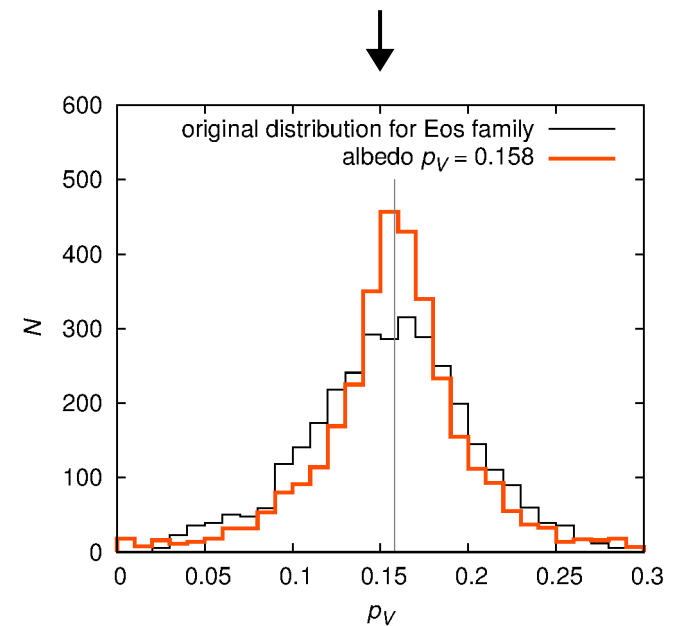
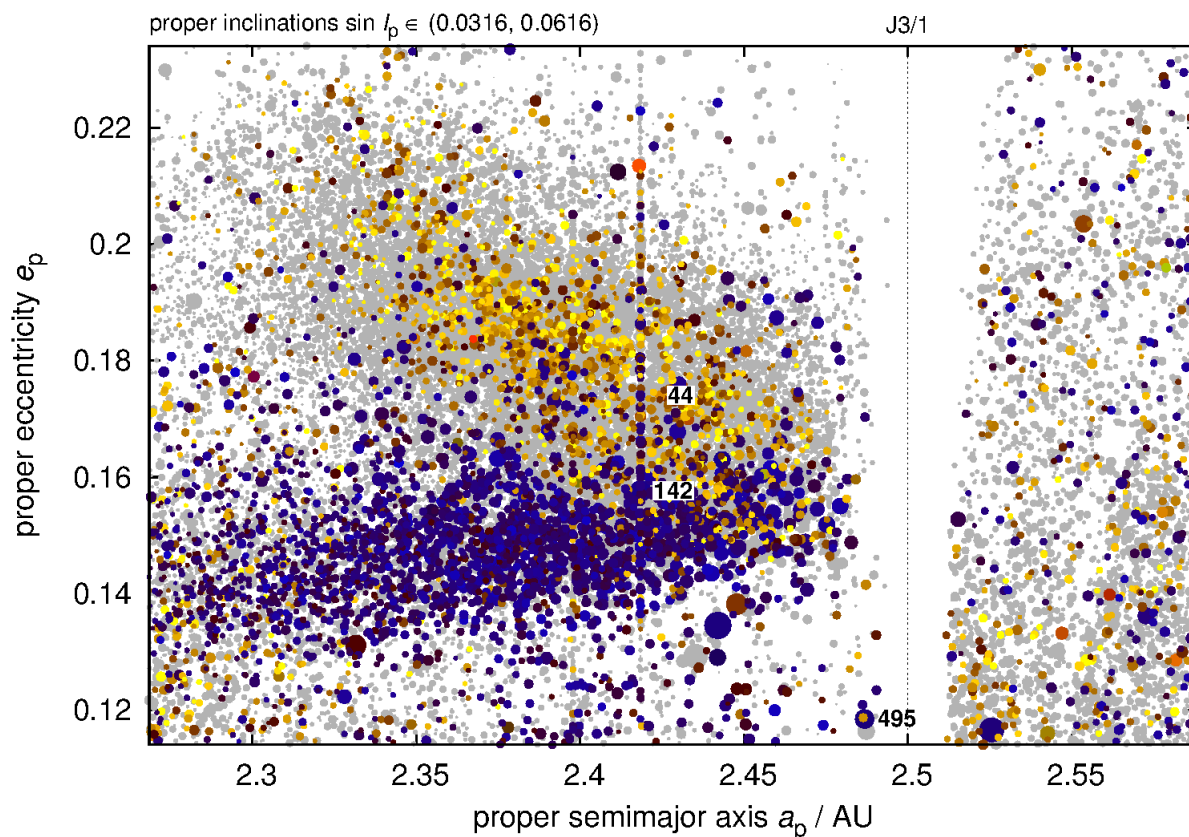
A number of unknowns...

i ... “mass-less” particles, j ... massive bodies

- $N_{\text{TP}}, \mathbf{r}_i, \mathbf{v}_i, \mathbf{r}_j, \mathbf{v}_j, m_i, m_j, \tau_{\text{mig}}, \Delta v, D_i, \rho_i, \rho_{\text{surf}}, K, C, A_{\text{Bond}}, \epsilon, c_{\text{YORP}}, \lambda_i, \beta_i, \omega_i, f_k, g_k, B, \beta_1, \beta_2, D_0, D_{\text{PB}}, \rho_{\text{PB}}, v_{\text{imp}}, \phi_{\text{imp}}, f_{\text{imp}}, \omega_{\text{imp}}$
- $q_a, q_b, q_c, D_1, D_2, n_{\text{norm}}, \rho_{\text{bulk}}, Q_0, a, B, b, q_{\text{fact}}, P_{ij}, v_{ij}, t_{\text{end}}, dN(t), dN(D,t)$
- **49** (!) a-priori unknown ICs and parameters
- not speaking about SPH models yet...
- beware of discretisation Δt

Uncertainty 1: Family membership

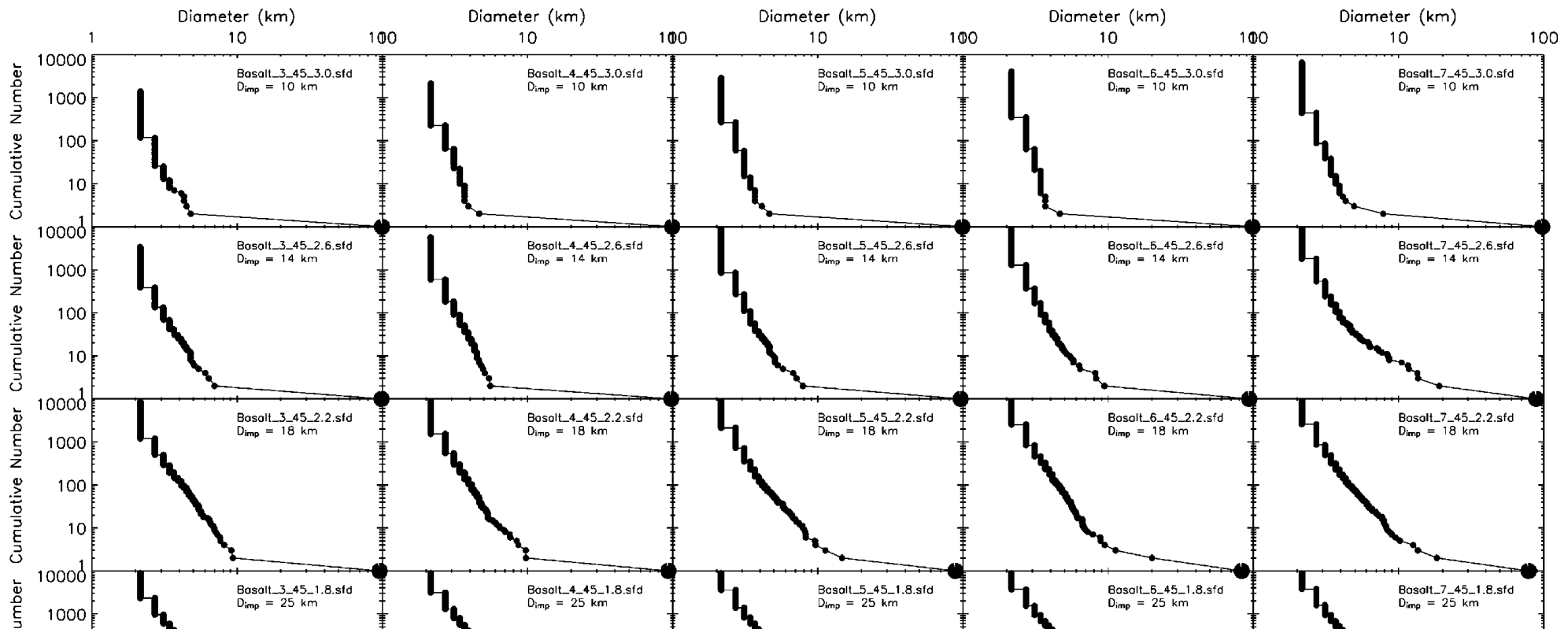
- missing physical data → one cannot exclude all interlopers
- a broad distribution of albedo even within *one* family



Milani & Knežević (2003)
Masiero et al. (2011)
cf. Dykhuis & Greenberg (2015)

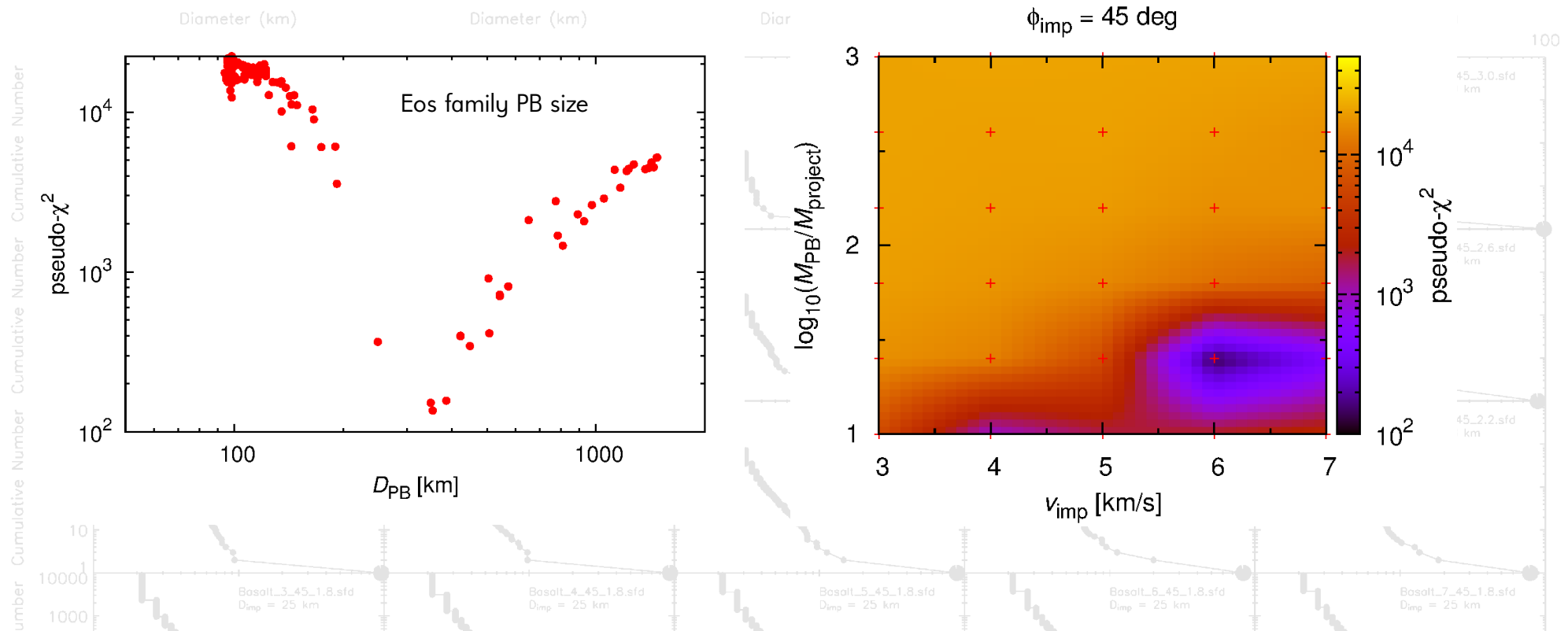
2: Parent-body size

- a simplified scaling (Durda et al. 2007), cf. Tanga et al. (1999)
- uncertainties: multiple fits have low χ^2 , interlopers
- systematics: number & distribution of SPH particles



3: Parent-body size

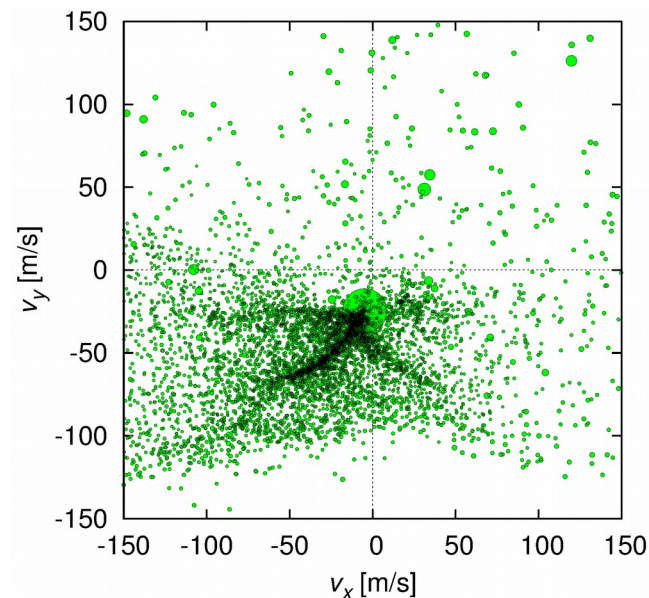
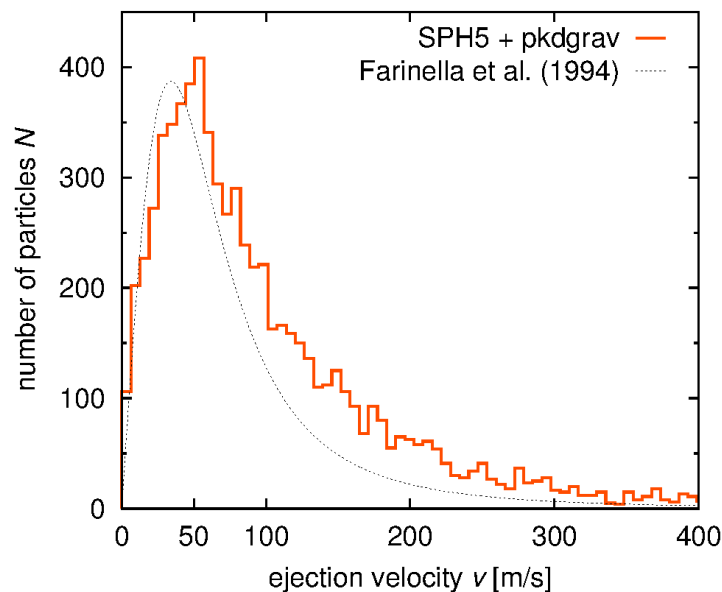
- a simplified scaling (Durda et al. 2007), cf. Tanga et al. (1999)
- uncertainties: multiple fits have low χ^2 , interlopers
- systematics: number & distribution of SPH particles



4: Initial velocity field

↓ e.g. Karin family (Nesvorný et al. 2006)

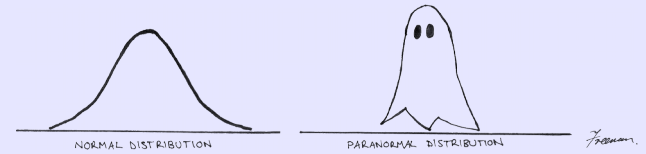
- usually, we assume *isotropic*, with a peak at v_{esc} from PB
- however, Veritas is *not* the case (Tsiganis et al. 2007)
- uncertainties: impact geometry ($f_{\text{imp}}, \omega_{\text{imp}}$)
- systematics: anisotropies (as indicated by SPH models)?



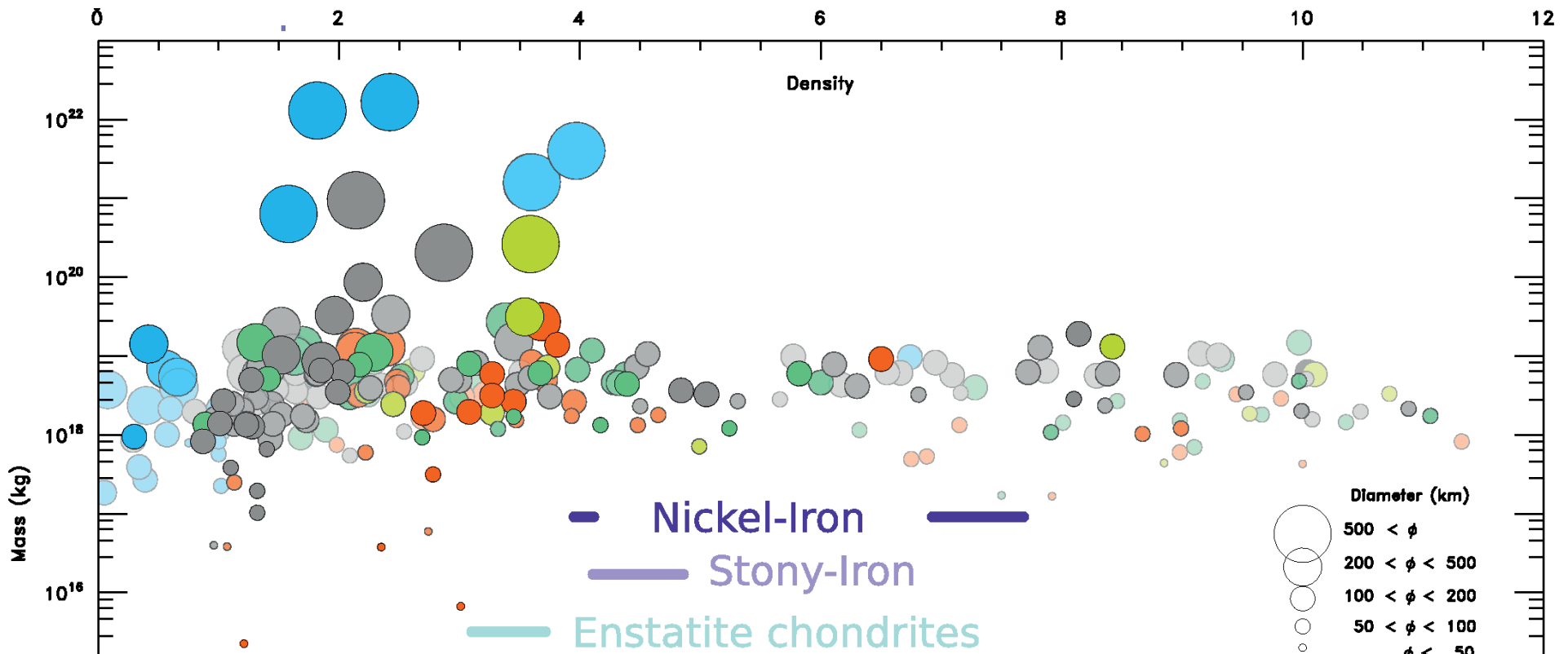
$D = 100$ km
 $d = 25$ km
 $v = 5$ km/s
 $\varphi = 45^\circ$
 $N_{\text{SPH}} = 10^4$

Benz & Asphaug (1994)
Richardson (2000)

5: Density

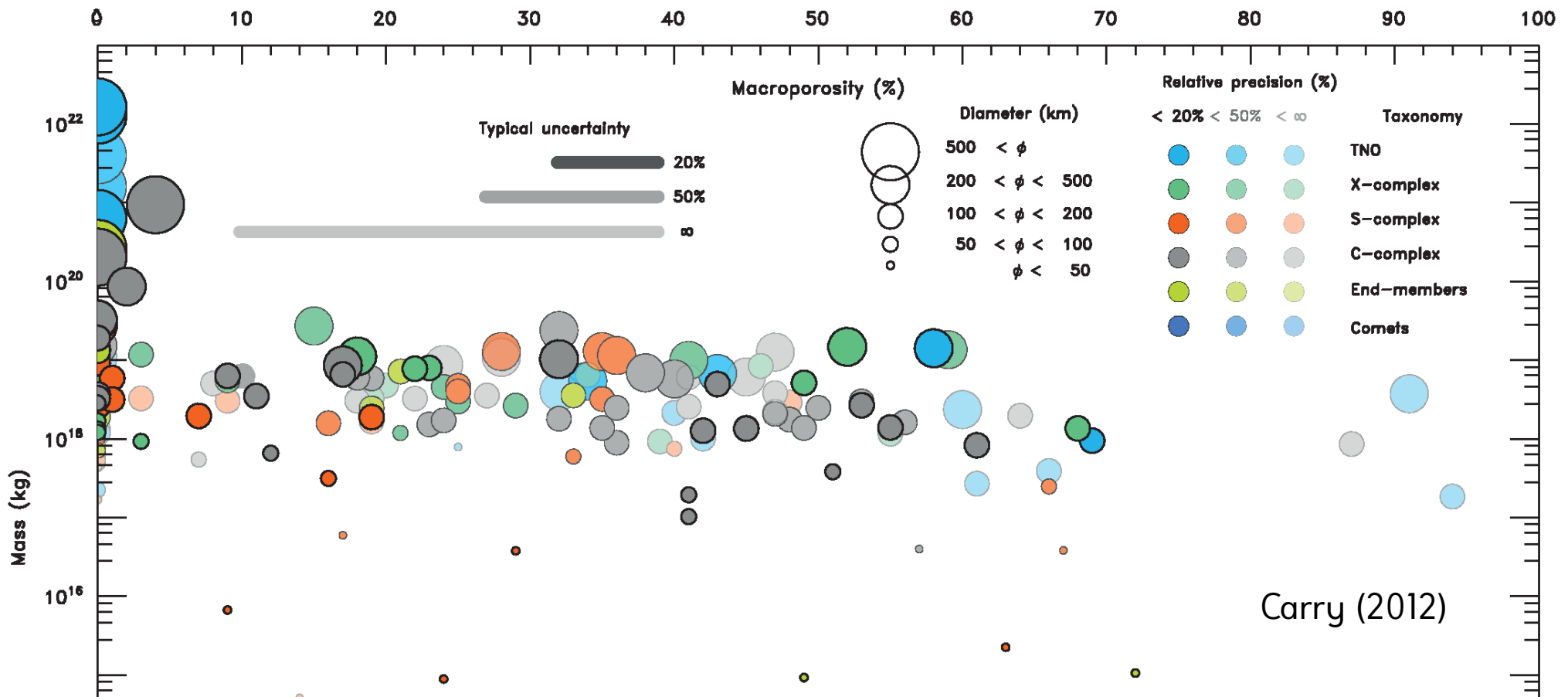


- distribution is *not* gaussian (see Carry 2012)
- low number of high-precision (20%) measurements
- possible systematics in volumes, calibration



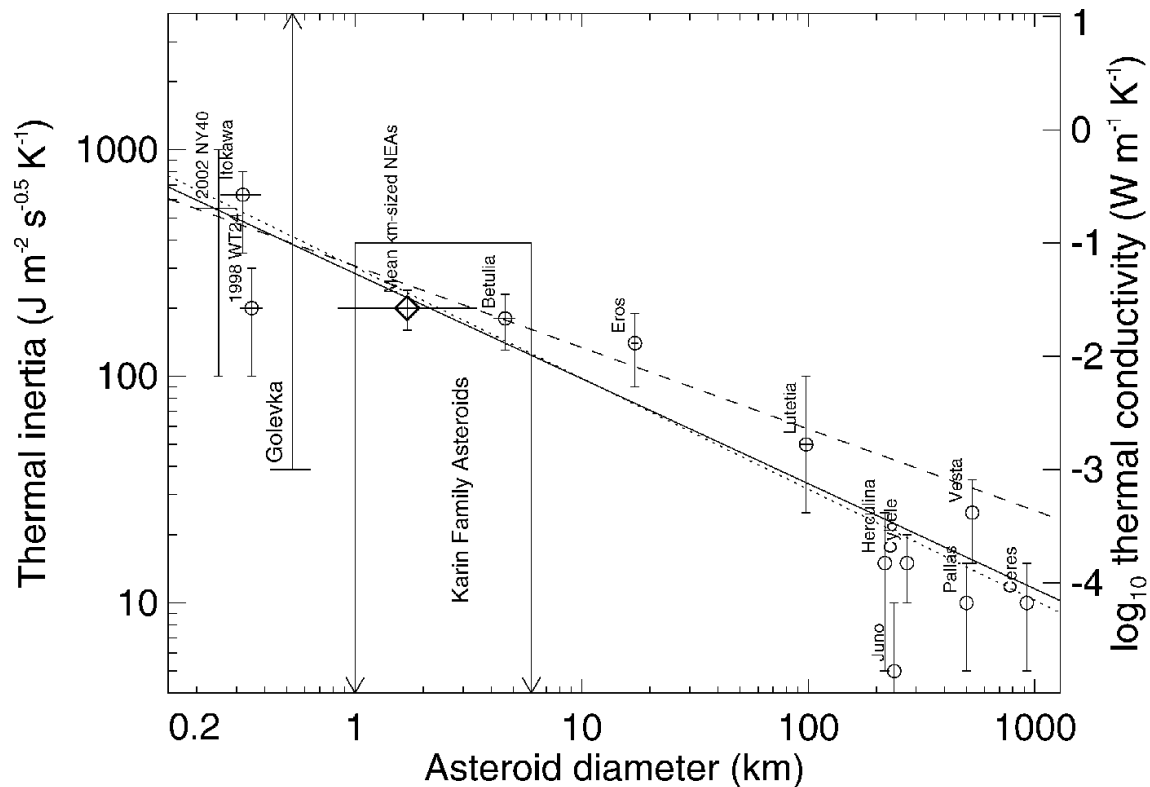
6: Porosity

- again, a low number of 20% measurements
- calibration problems if the value for (101955) Bennu is used



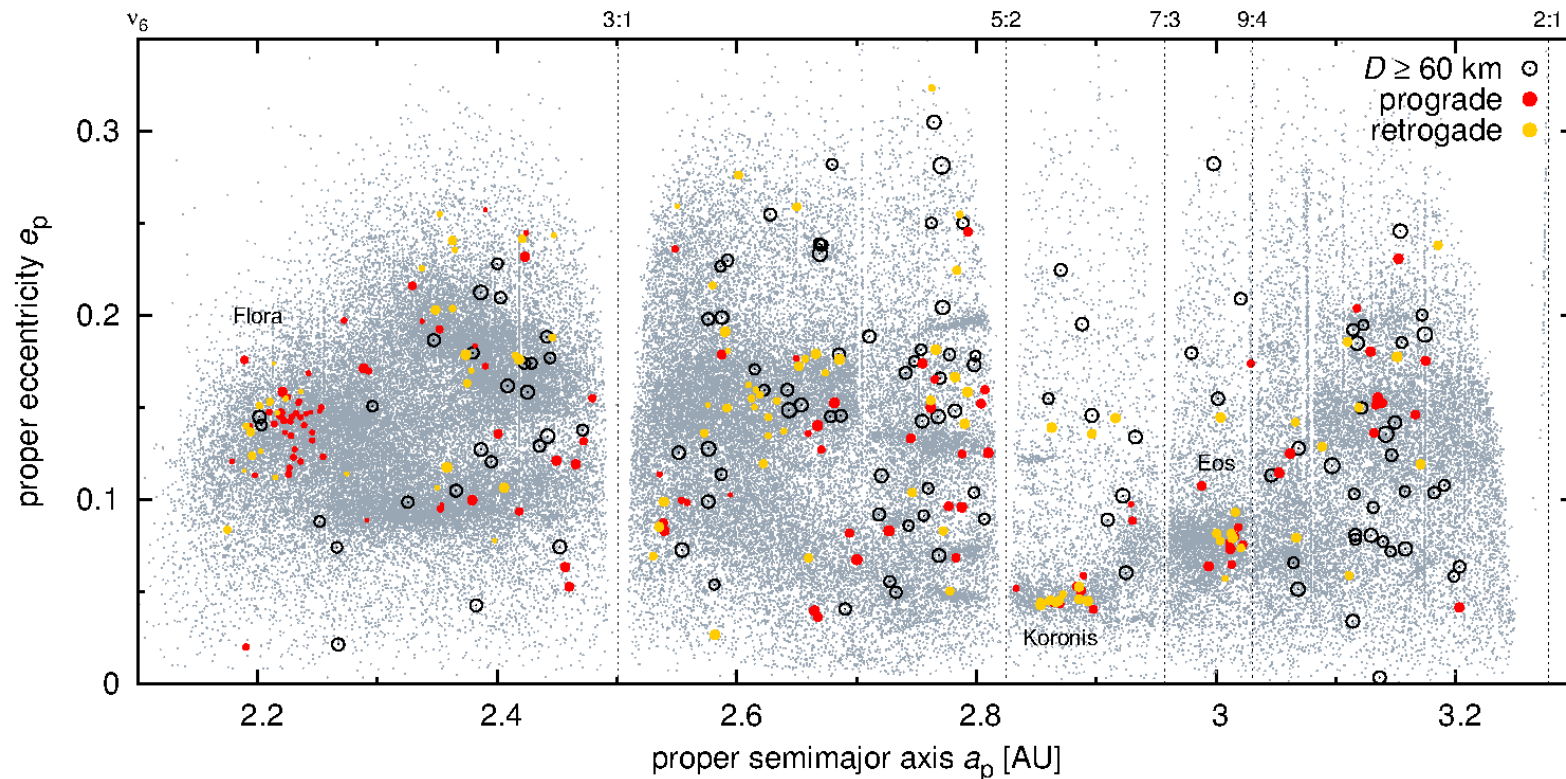
7: Thermal conductivity

- trend vs step-like function? (cf. Delbó et al. 2007)
- uncertainty: a correlation of K & ρ_{surf}
- systematics: NEATM model for spheres (not shapes)



8: Spin

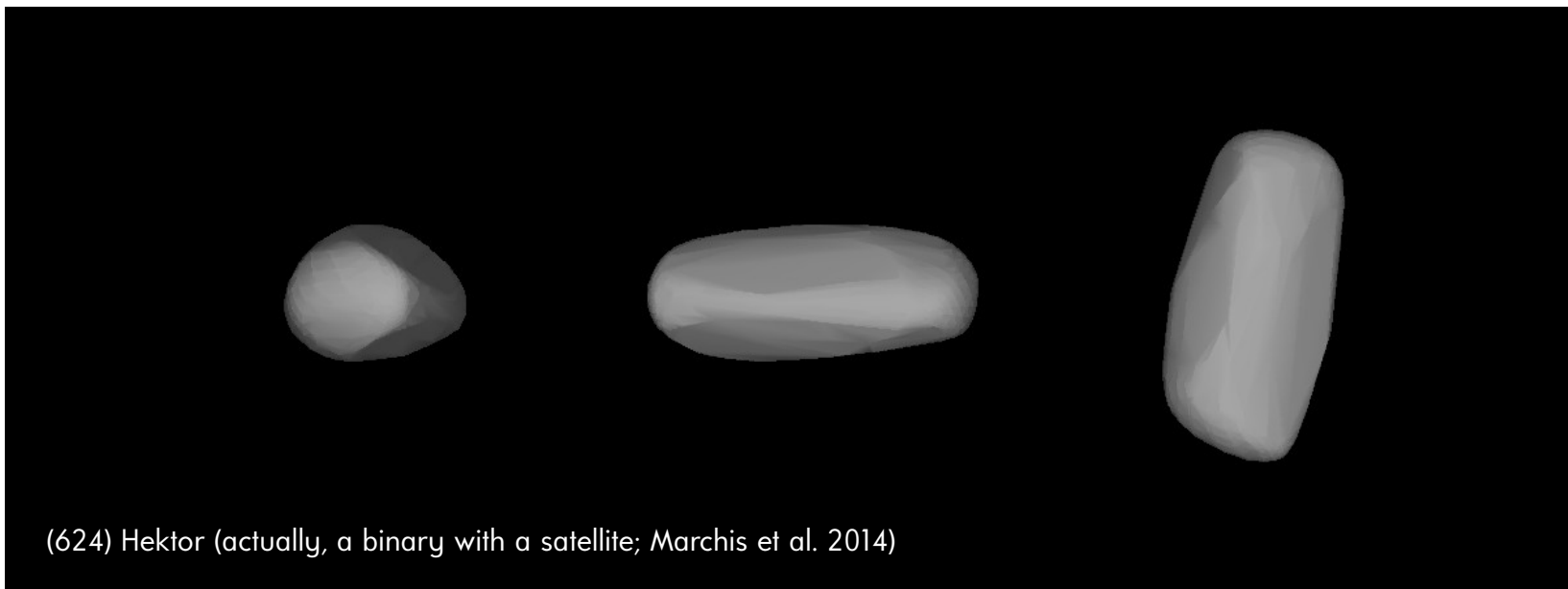
- usually assumed isotropic & maxwellian rates ω
- DAMIT database (Hanuš et al. 2013), uncertainties 10° , multiple solutions in λ , systematics in λ ? (Bowell et al. 2014)



9: Shape

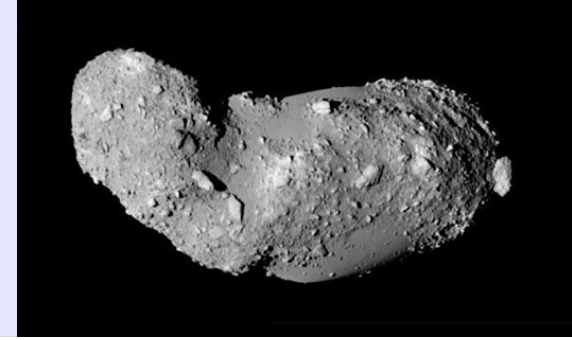
Well, only a model of...

- a correspondence to *real* shapes?
- YORP torques (Čapek & Vokrouhlický 2004) for a set of gaussian random “spheres” ← random assignment
- small-scale topography is important (Statler 2009)
- stochastic YORP (Bottke et al. 2014, Cotto-Figueroa et al. 2014)



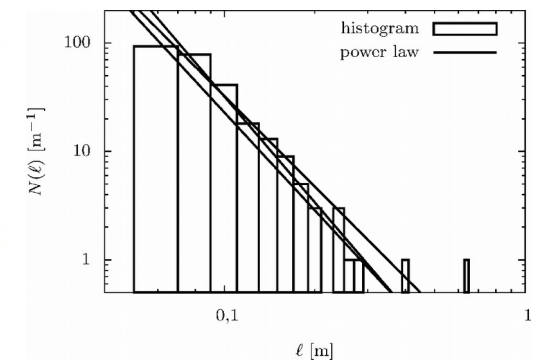
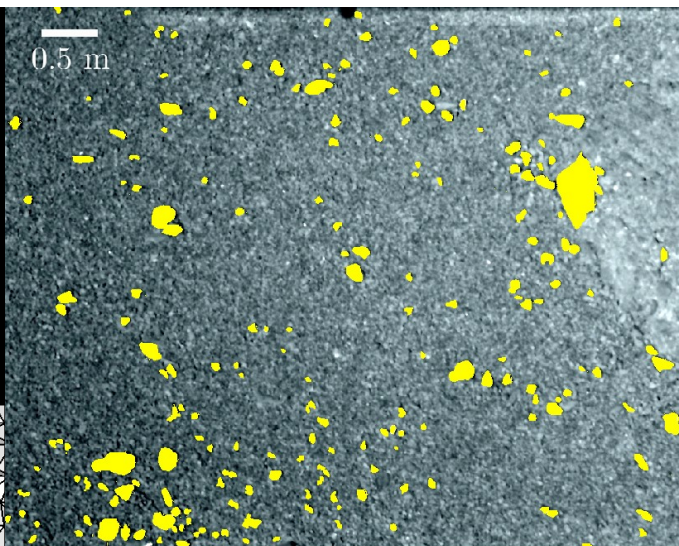
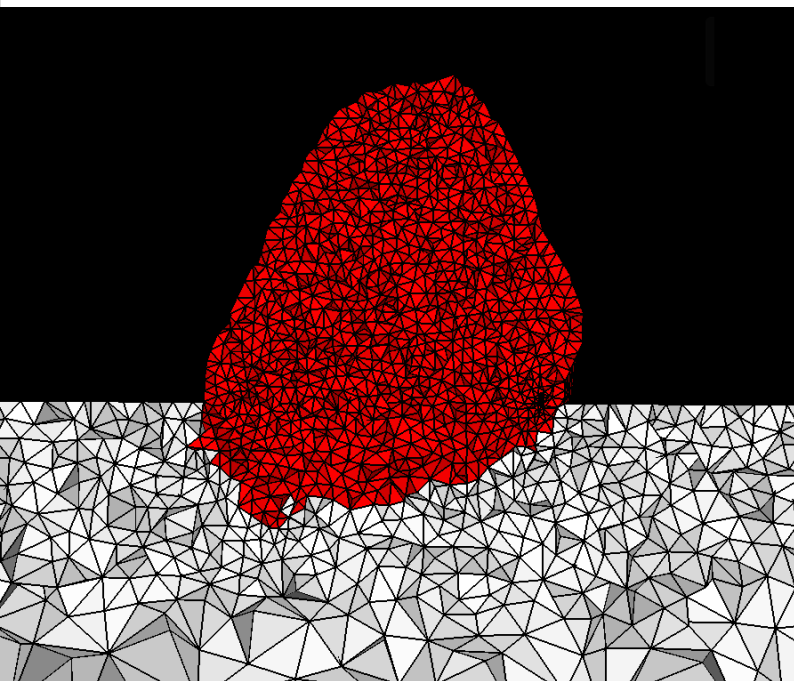
(624) Hektor (actually, a binary with a satellite; Marchis et al. 2014)

Individual 10: Boulders



- 3-dimensional heat diffusion (Golubov & Krugly 2012, Ševecek et al. submit.) → non-negligible YORP torques
- uncertainties: SFD of boulders, thermal parameters
- systematics: real shapes

cf. Lowry et al. (2014)



$d\omega/dt \sim 10^{-7} \text{ rad day}^{-2}$
for (25143) Itokawa

Figure 6. The image ST_2563607030_v (Saito et al. 2010) with highlighted boulders from which we derived their size distribution, for the computation of the total torque.

Finite element method

- Ševeček et al. (submit.), notation Langtangen (2003):

$$\mathcal{L} \equiv \rho C \partial_t - \nabla \cdot K \nabla, \quad \mathcal{L}(u) = 0. \quad K \partial_n u + \epsilon \sigma u^4 = (1 - A) \Phi \vec{s} \cdot \vec{n},$$

↓ FEM

$$u \doteq \hat{u} = \sum_{j=1}^M u_j N_j,$$

$$\int_{\Omega} \rho C \partial_t \hat{u} N_i d\Omega - \int_{\Omega} \nabla \cdot (K \nabla \hat{u}) N_i d\Omega = 0.$$

↓ Green lemma

$$\int_{\Omega} \nabla \cdot (K \nabla \hat{u}) N_i d\Omega = - \int_{\Omega} K \nabla \hat{u} \cdot \nabla N_i d\Omega + \int_{\partial\Omega} K \partial_n \hat{u} N_i d\Gamma,$$

↓ discretisation, BC, linearisation

$$\int_{\Omega} \mathcal{L}(\hat{u}) N_i d\Omega = 0.$$

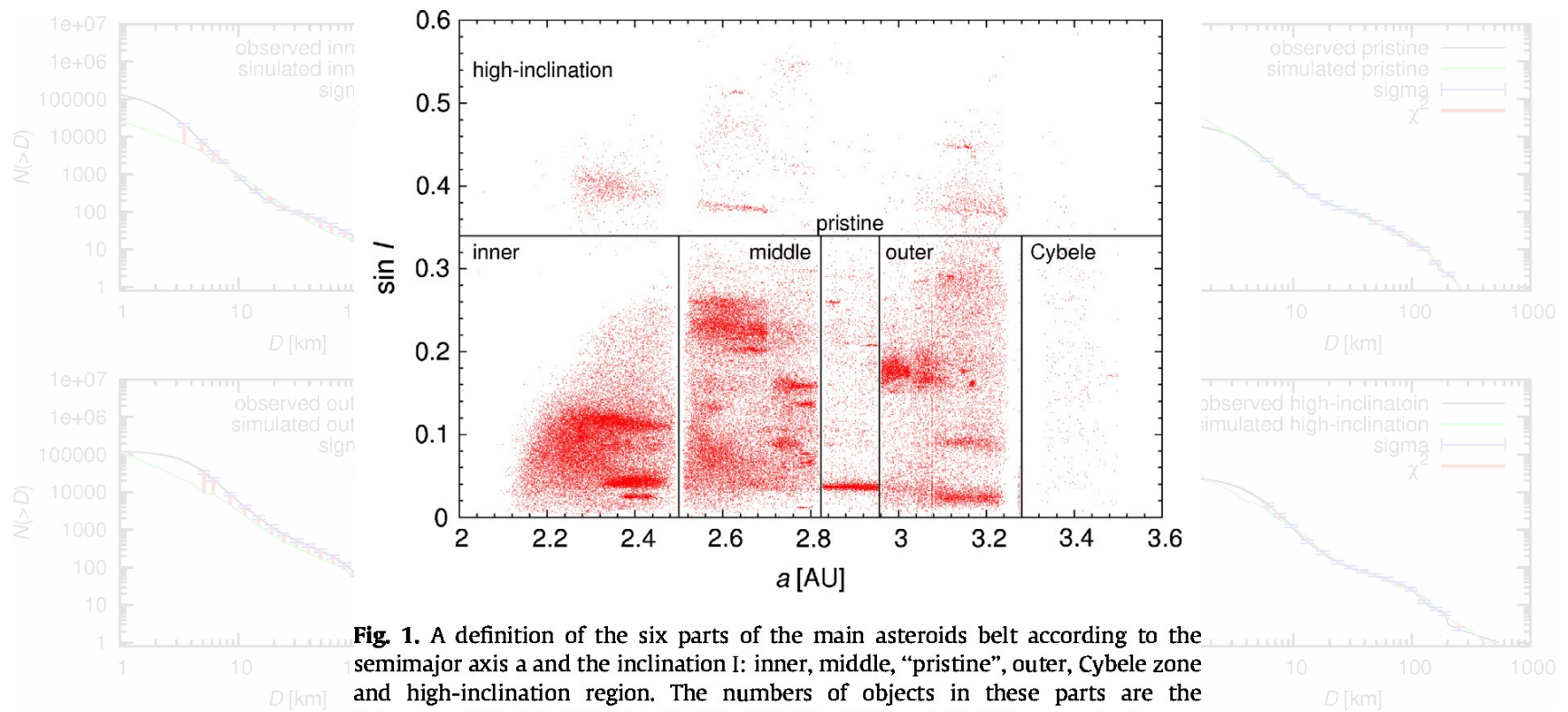
$$\int_{\Omega} \frac{\rho C}{\Delta t} \hat{u}^n N_i d\Omega - \int_{\Omega} \frac{\rho C}{\Delta t} \hat{u}^{n-1} N_i d\Omega + \int_{\Omega} K \nabla \hat{u} \cdot \nabla N_i d\Omega +$$

weak formulation
Galerkin method

$$+ \int_{\partial\Omega} \epsilon \sigma (\hat{u}^{n-1})^3 \hat{u}^n N_i d\Gamma - \int_{\partial\Omega} (1 - A) \Phi \vec{s} \cdot \vec{n} N_i d\Gamma = 0.$$

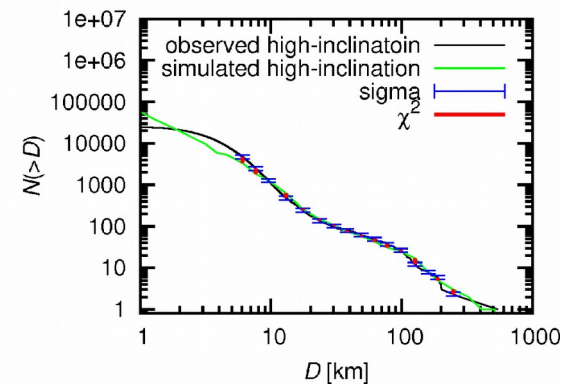
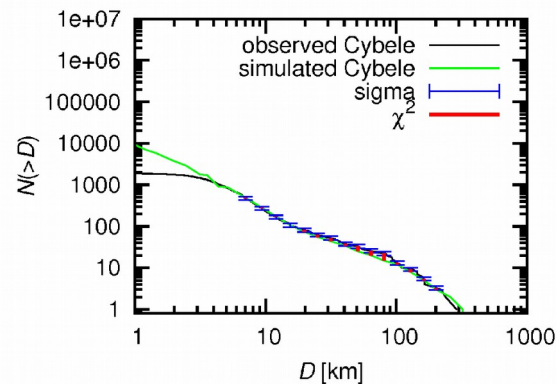
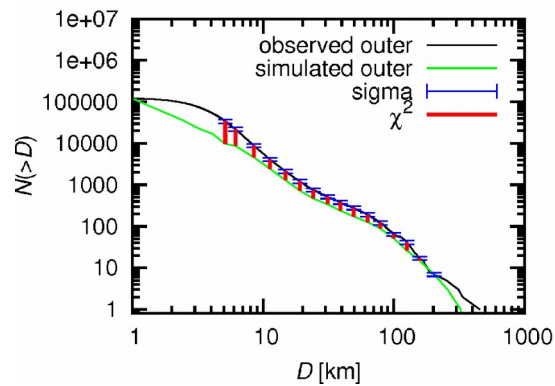
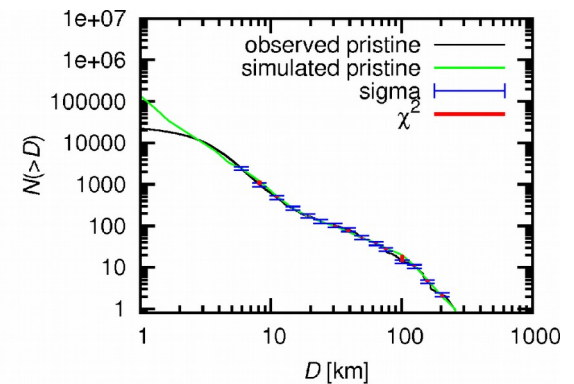
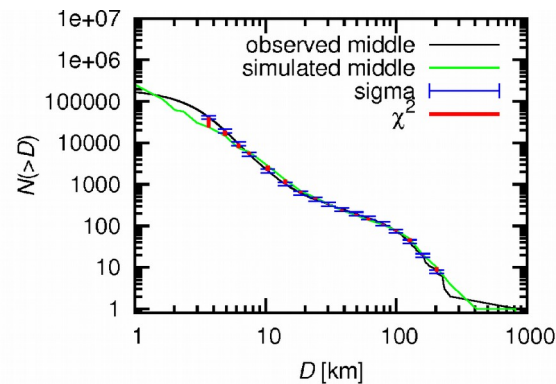
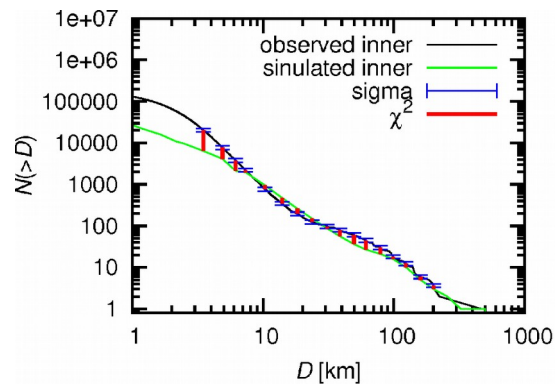
11: Internal structure

- monolith vs macro- vs microscopic porosity (Benz & Asphaug 1999, Benavidez et al. 2012, Jutzi et al. 2014)
- stochastic evolution for 6 MB parts (Cibulková et al. 2014)



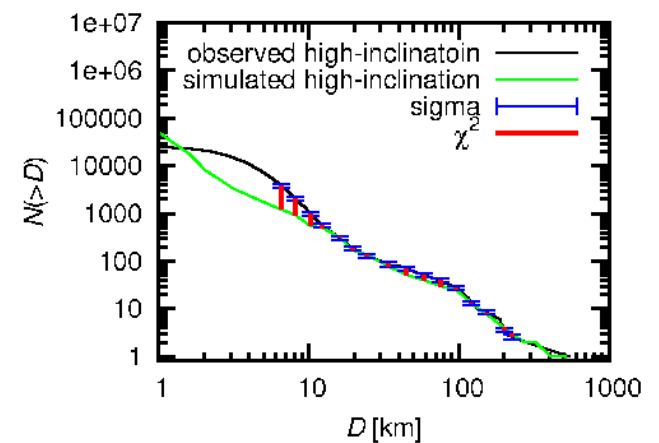
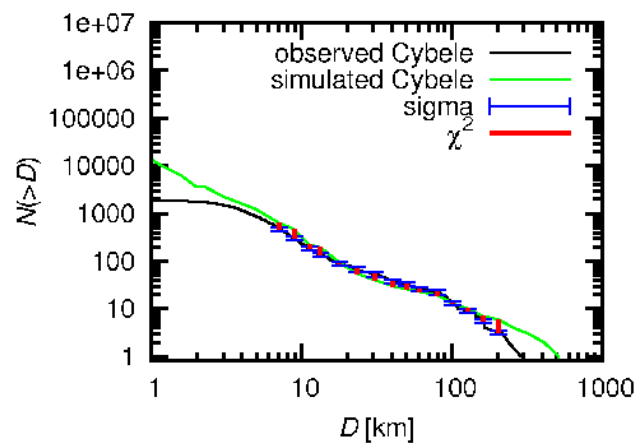
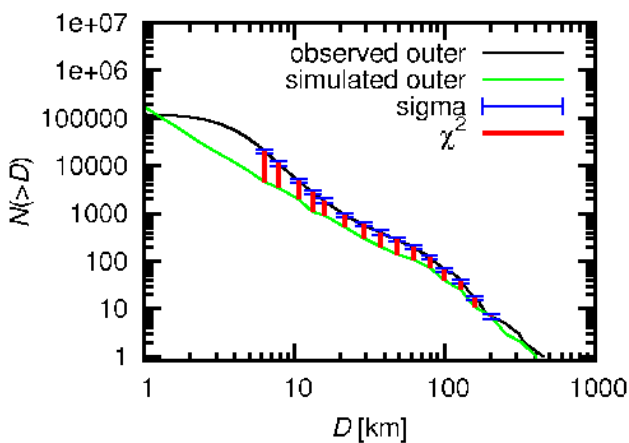
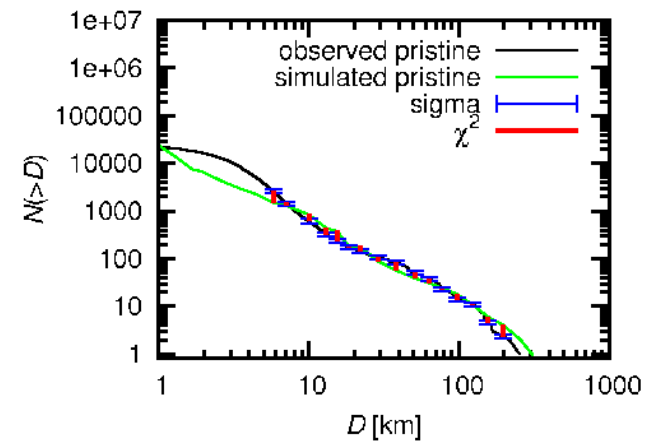
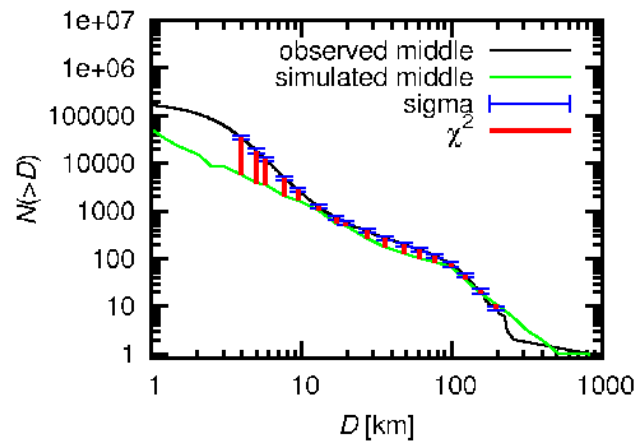
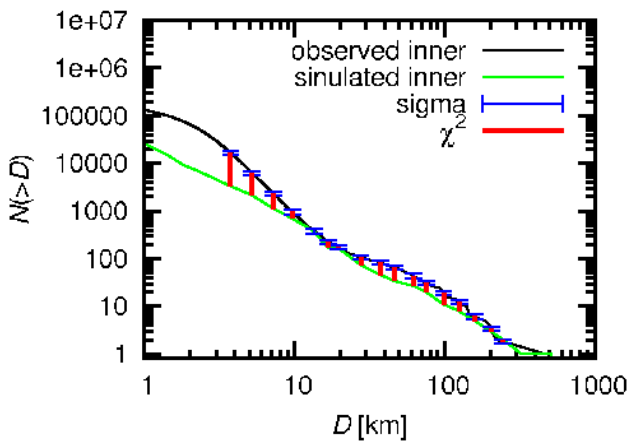
11: Internal structure

- monolith vs macro- vs microscopic porosity (Benz & Asphaug 1999, Benavidez et al. 2012, Jutzi et al. 2014)
- stochastic evolution for 6 MB parts (Cibulková et al. 2014)



Internal structure (cont.)

- macroporous rubble piles too weak (Cibulková et al. 2014)



12: Scaling law

i.e. strength in erg/g vs radius* $Q_D = Q_0 r^a + B \rho r^b$

- uncertainties: material parameters ← a factor of 2?
- systematics: velocity dependence (Steward & Leinhardt 2009), impact angle scaling (Jutzi et al. 2014)
- total damage of the parent body (Michel et al. 2003)
→ dust production?
- bouncing and friction during gravitational reaccumulation (Richardson et al. 2009)
- chemical reactions in gaseous phase (i.e. not a simple EOS of Tillotson 1962, Melosh 2000)

13: Migration scenario

- jumping-Jupiter (Morbidelli et al. 2010), fifth giant planet (Nesvorný 2011)
- sufficient sampling ~ 1 yr for x, y, z interpolation
- uncertainties: M_{disk}
- systematics: different scenario, late phases, resonance sweeping, additional populations? (E-belt, Bottke et al. 2011)

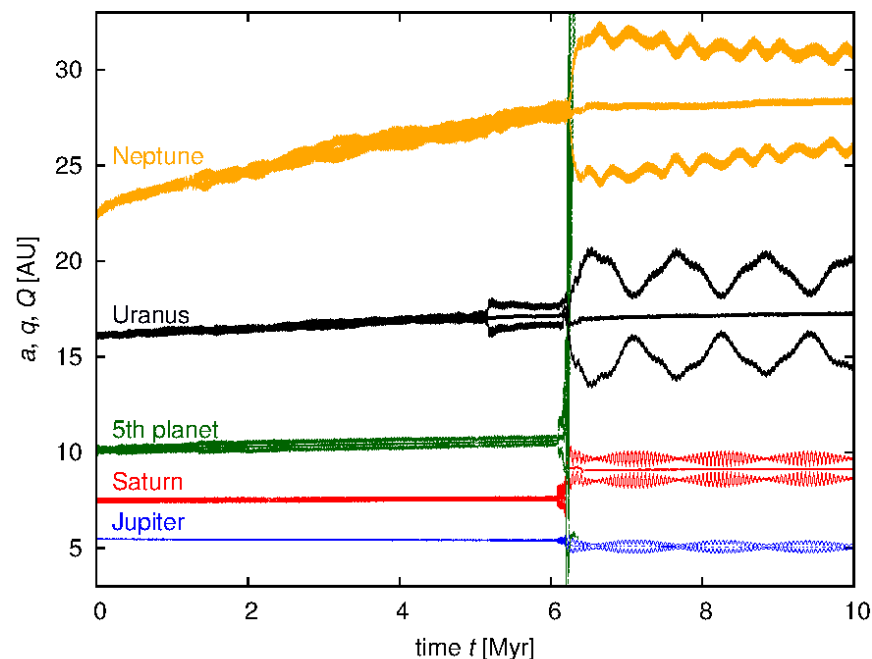


Figure 5. Orbital evolution of giant planets in the fifth giant planet scenario, adopted from Nesvorný & Morbidelli (2012), during the jumping Jupiter instability, as it was reproduced by our modified integrator. We plot time t vs the semimajor axis a , the pericentre q and the apocentre Q . Each evolutionary track is labeled with the name of the corresponding giant planet.

Chrenko et al. (in prep.)

14: Dynamical decay

- Minton & Malhotra (2010), a simple reconfiguration only
- uncertainties: collisional $p_i(t)$, $v_{\text{imp}}(t)$ for different scenarios
- systematics: an estimate of primordial population

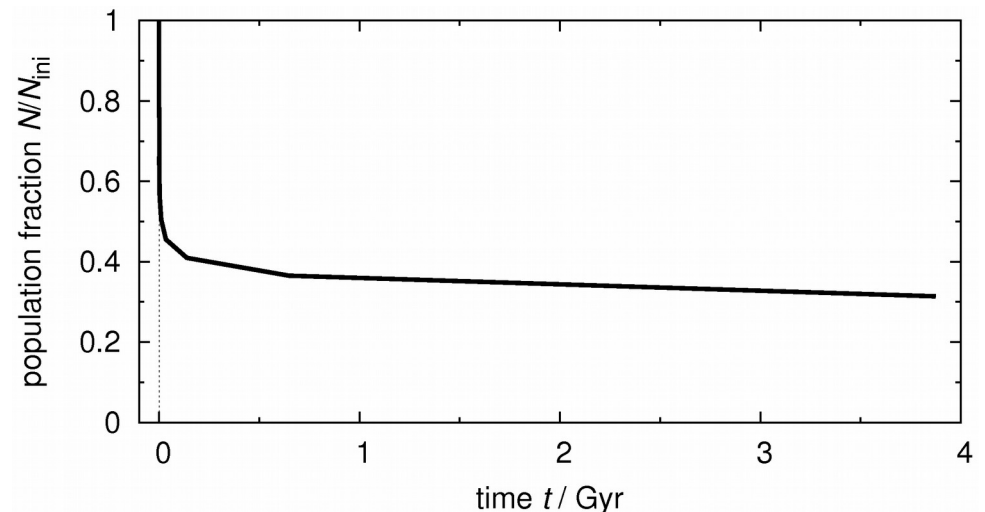
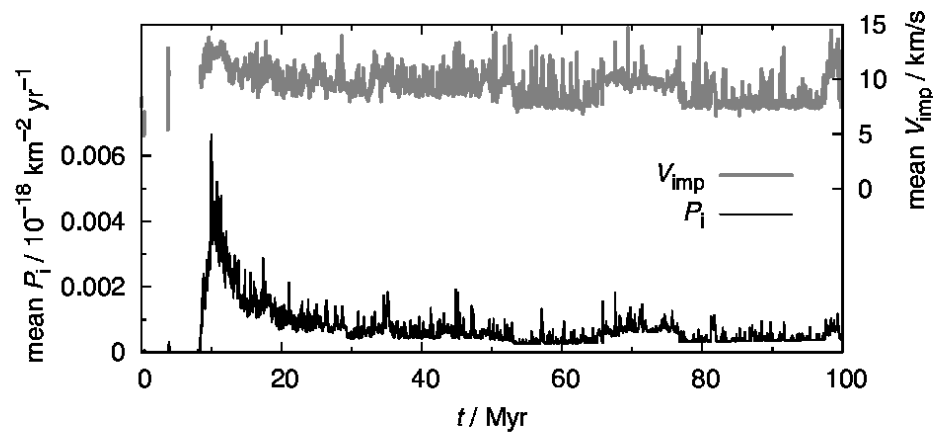


Fig. 6. Temporal evolution of the intrinsic collisional probability P_i (bottom) and mean collisional velocity V_{imp} (top) computed for collisions between cometary-disk bodies and the main belt asteroids. The time $t = 0$ is arbitrary here; the sudden increase in P_i values corresponds to the beginning of the LHB.

15: Size distribution of comets

- uncertainties: M_{disk} , slope(s) of the SFD for small D
- systematics: cratering on satellites, capture of Trojans, ...

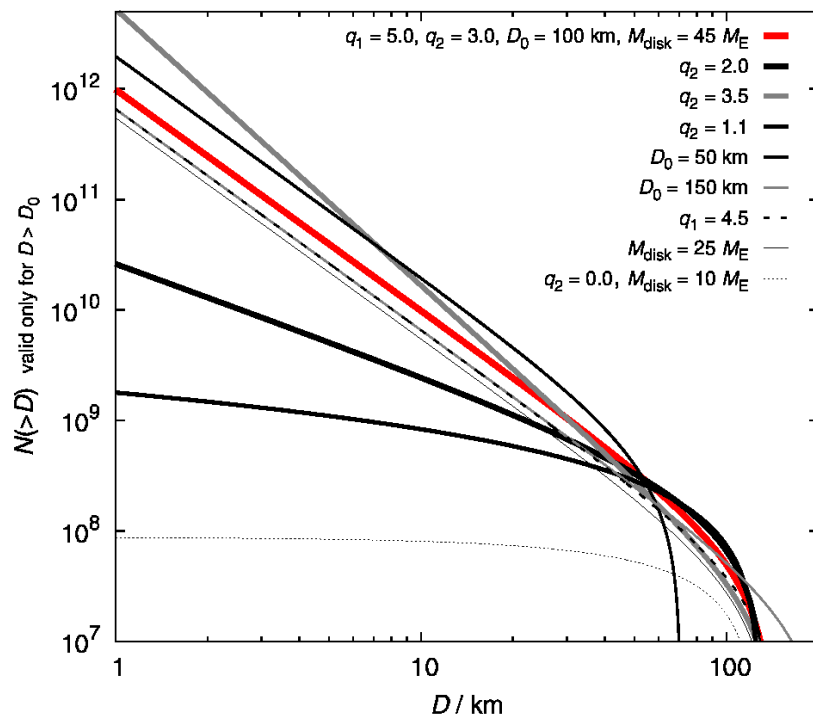


Fig. 7. Cumulative SFDs of the cometary disk tested in this work. All the parameters of our nominal choice are given in the top label; the other labels just report the parameters that changed relative to our nominal choice

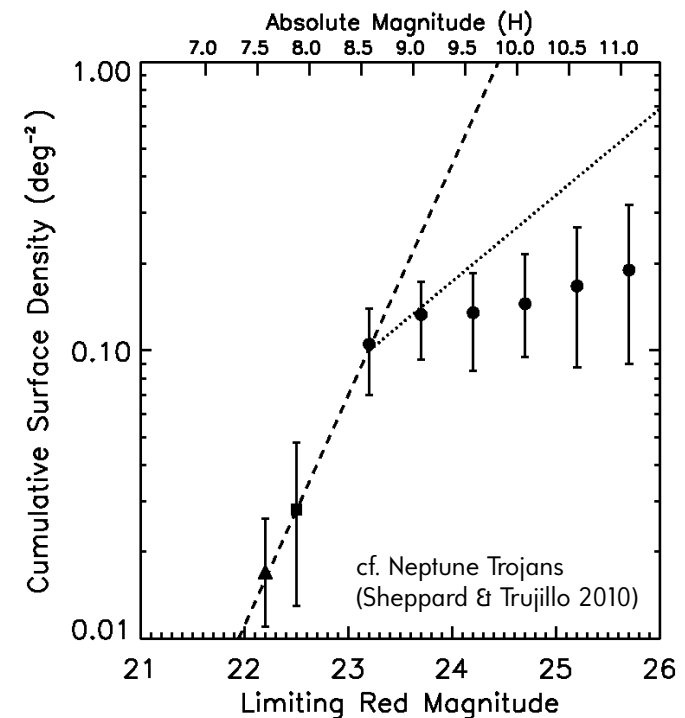
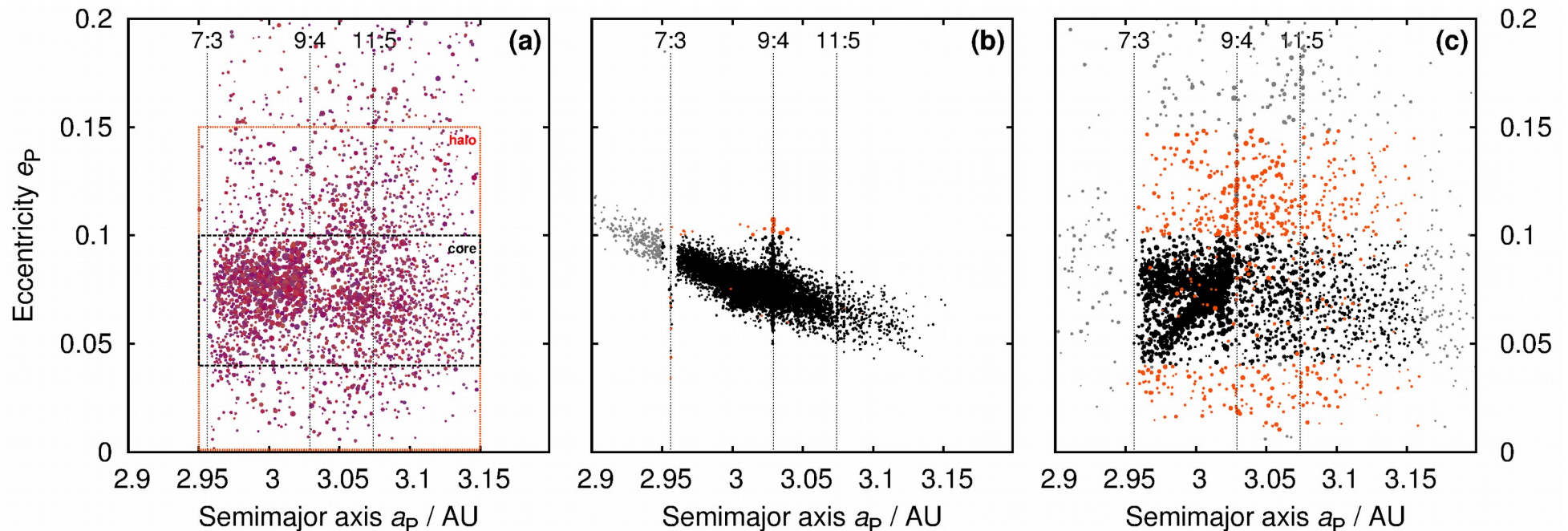


Figure 2. Cumulative luminosity function (CLF) of the Neptune Trojans, where the black circles are this work, the square is from the Deep Ecliptic Survey (DES; Chiang et al. 2003) and the triangle is from the Sloan Digital Sky Survey (SDSS; Becker et al. 2008). A steep power-law slope ($\alpha = 0.8 \pm 0.2$ ($q = 5 \pm 1$)), which

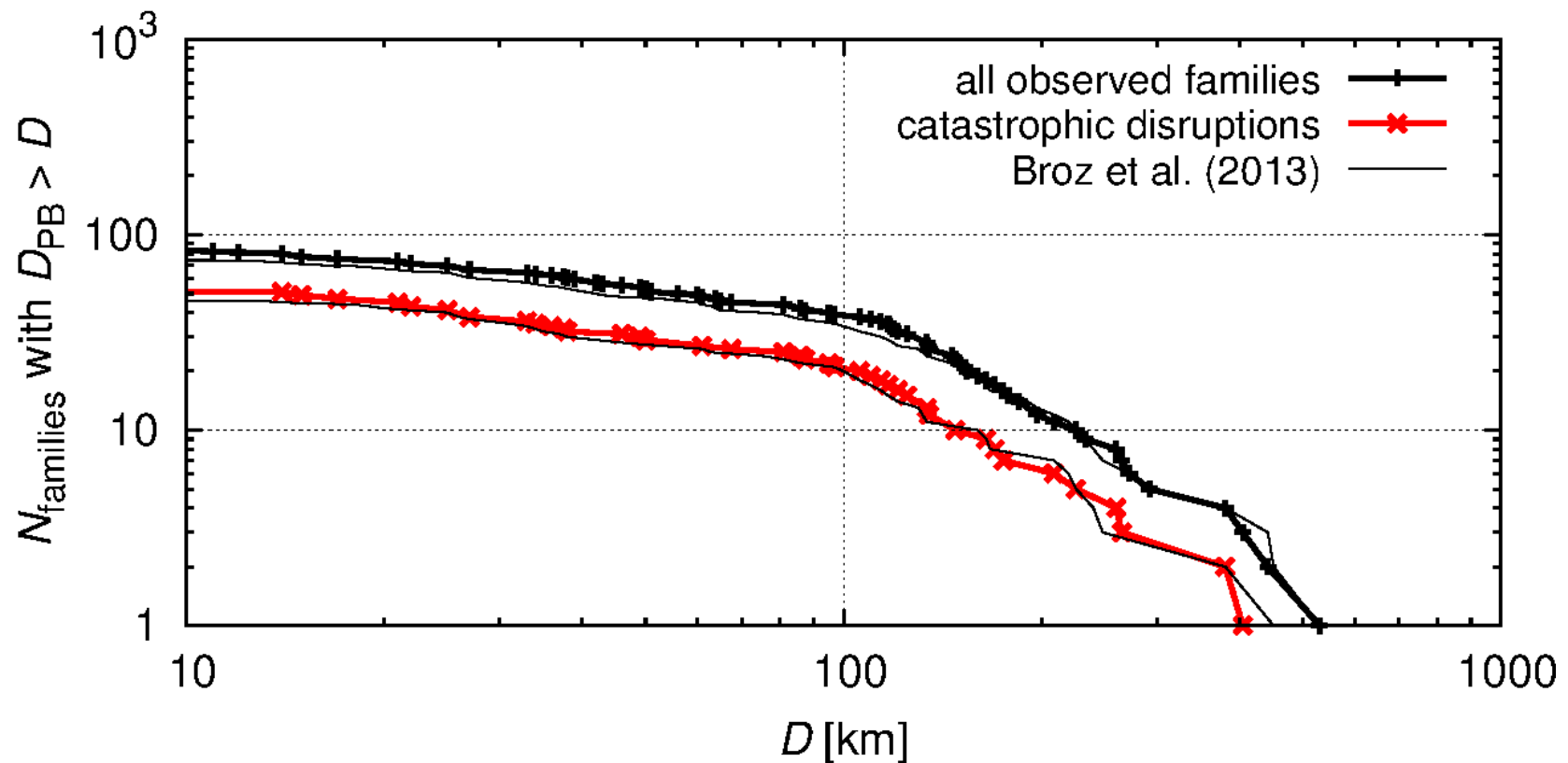
Application A: Individual families

- Eos (Brož & Morbidelli 2013), Euphrosyne (Carruba et al. 2014) → N -body models may guide family identifications
- core vs halo, distinct K-type taxonomy, gaps and scattering due to resonances, background often *not* uniform



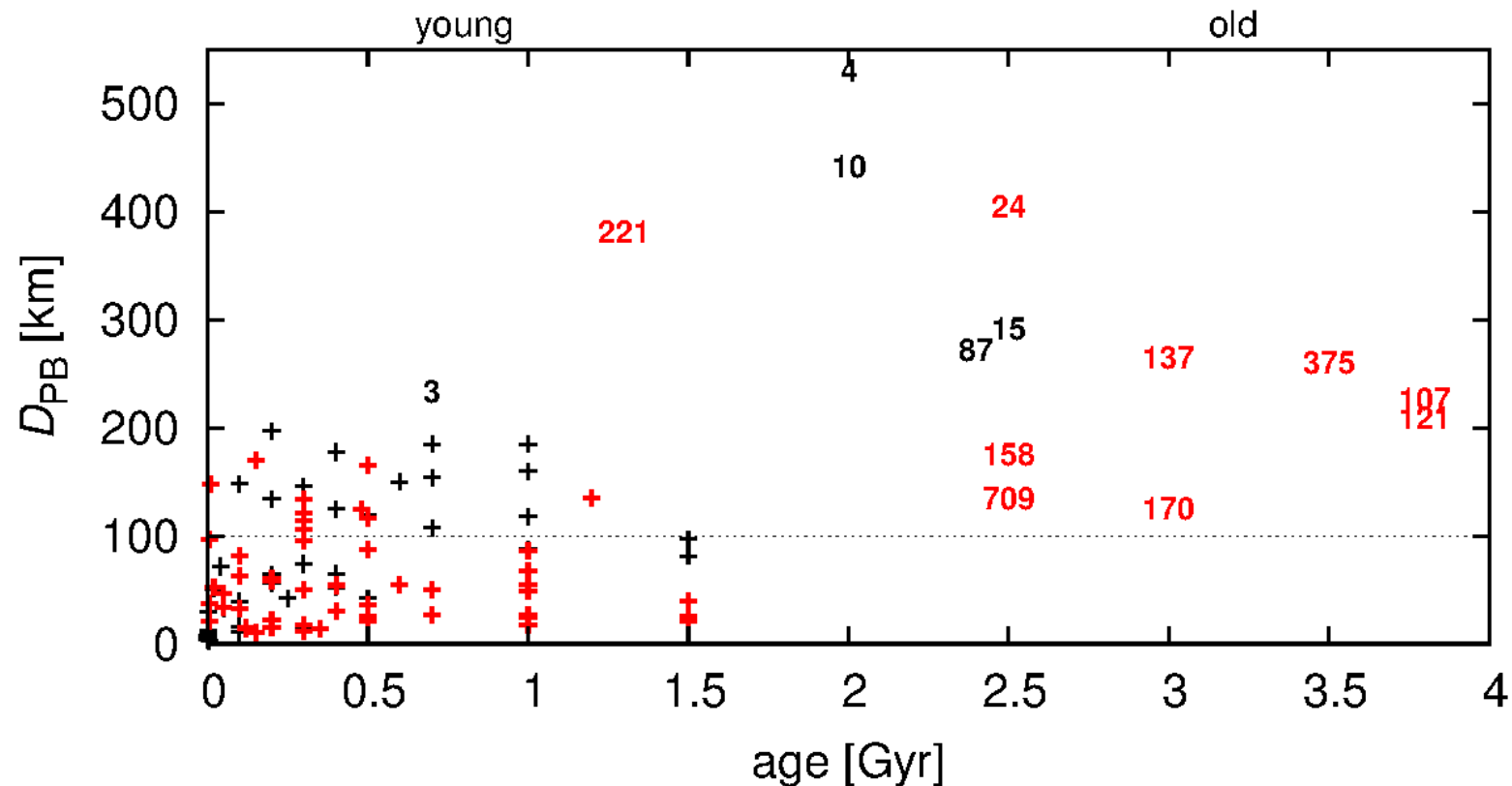
B: Statistics of families

- production function (Brož et al. 2013, Bottke et al. 2015)
- new families mostly $D_{PB} < 100$ km or craterings



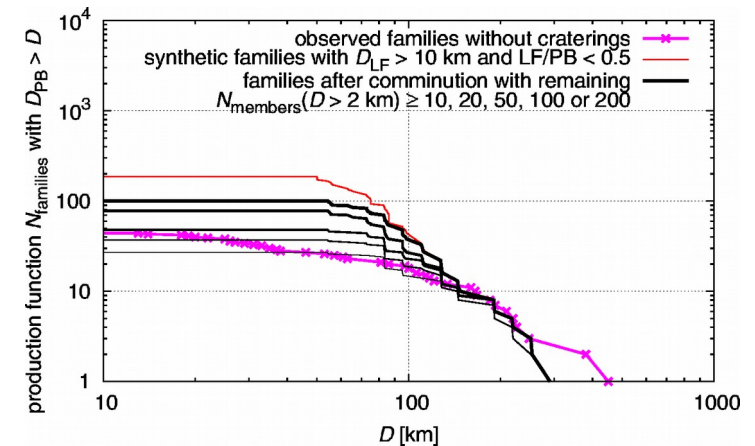
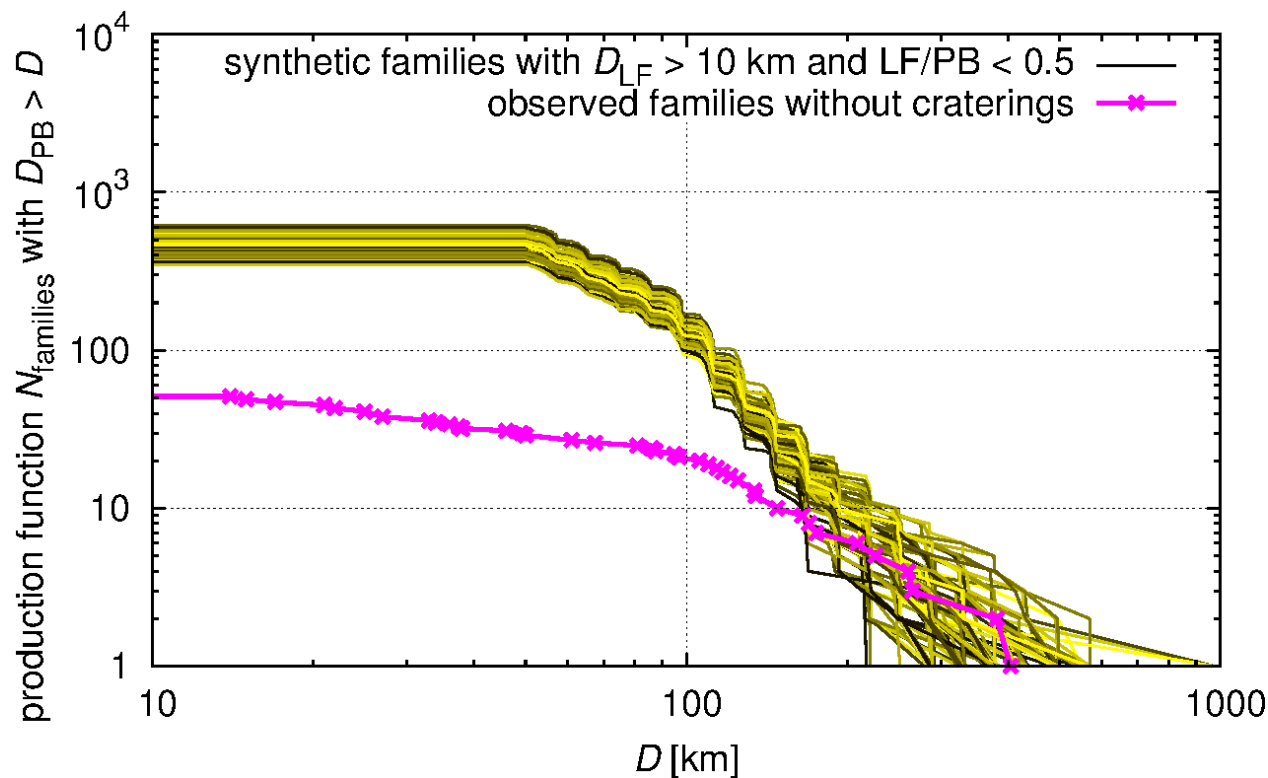
C: Ages of families

- dynamical ages span the *whole* interval of 4 Gyr
- *but* a depletion of old $D_{PB} < 100$ km families



D: Late heavy bombardment of the MB

- no problems producing $D_{PB} > 200$ km families (Brož et al. 2013)
- but 5 times more $D_{PB} > 100$ km families ← comminution and breakups of comets at low q



So called **E: Ghost families?**

- “pristine zone” ($a = 2.825$ to 2.955 AU), low background
- some families (e.g. Itha) have very shallow SFD, i.e. remnants of large/old/communioned families?

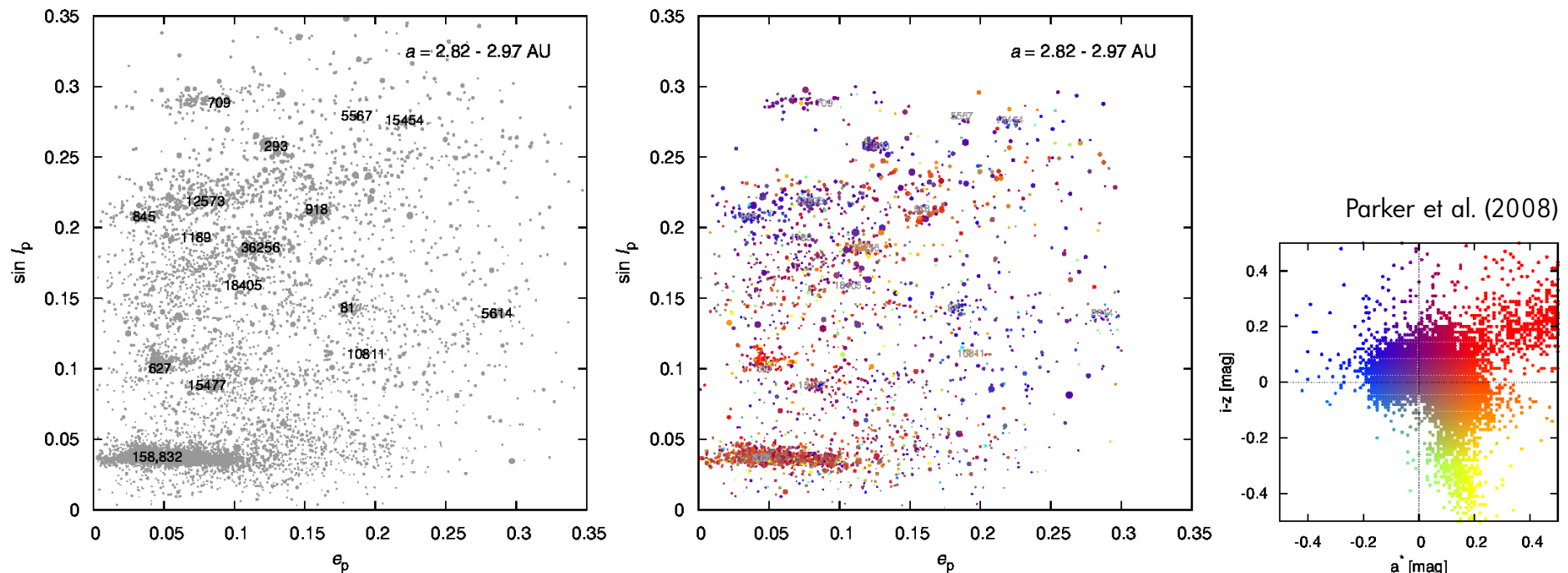
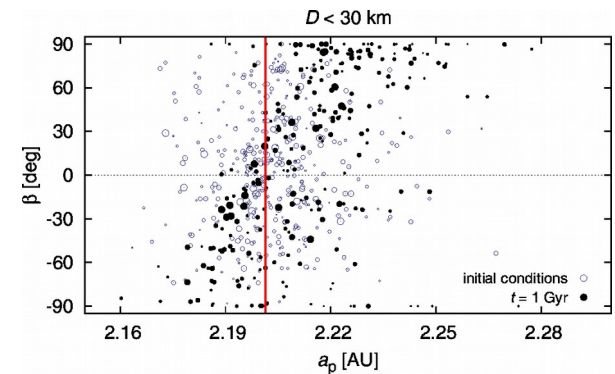
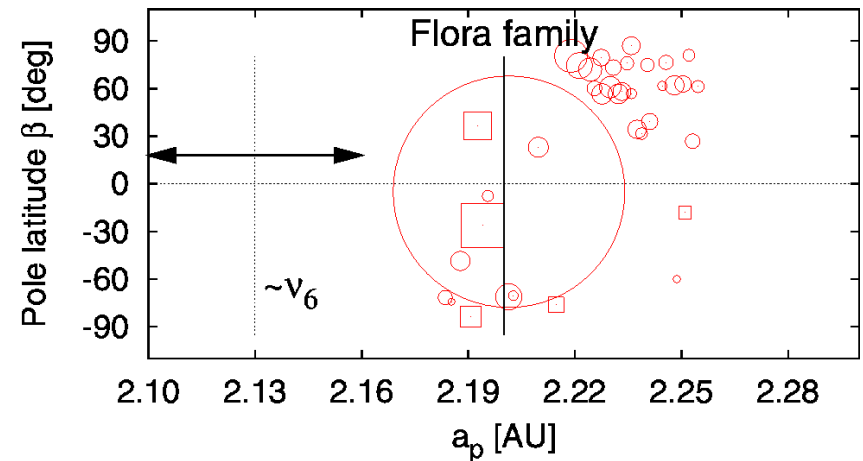
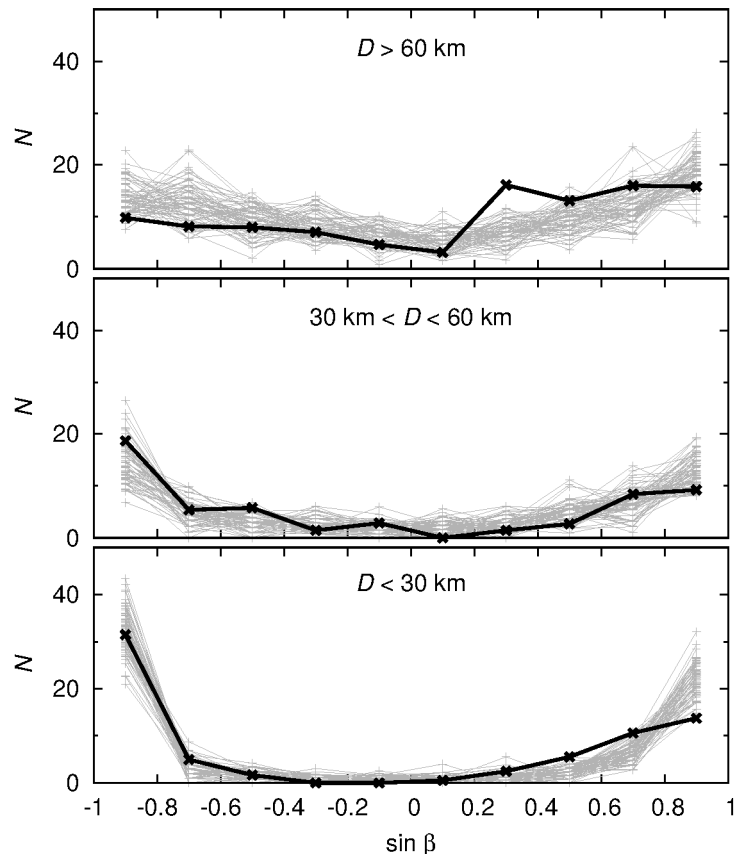


Fig. 12. “Pristine zone” of the main belt ($a_p = 2.825$ to 2.955 AU) displayed on the proper eccentricity e_p vs. proper inclination $\sin I_p$ plot. *Left panel:* the sizes of symbols correspond to the sizes of asteroids, the families are denoted by designations. *Right panel:* a subset of bodies for which SDSS data are available; the colours of symbols correspond to the SDSS colour indices a^* and $i - z$ (Parker et al. 2008).

F: New observables

(Hanuš et al. 2013)

- distribution of pole latitudes β for the whole MB \leftarrow YORP etc.
- not yet enough bodies for individual families, e.g. Flora



Conclusions

- no *strong* indication that thermal parameters are offset
- no model should rely on individual family membership
- bulk density is the most important (uncertain) parameter
- account for YORP due to boulders for sub-km asteroids
- there might be “ghost” families, remnants of LHB
- essentially no constraints for breakups of comets

Future applications



Blue Eye 600 robotic observatory

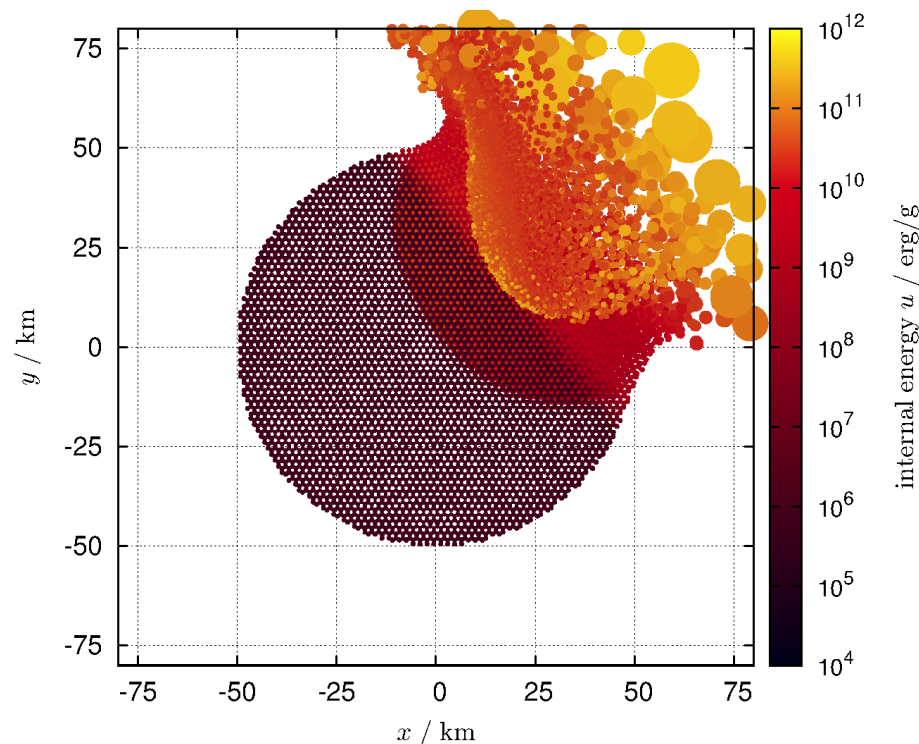
- “brute force” approach → new poles for family members
cf. <http://www.projectsoft.cz/en/roboticka-observator.php>
- observations of sub-km family members by surveys
- new NEO model (Granvik et al., in prep.) → its SFD as a strong constraint
- SFD of Neptune Trojans → constraints for comets
- N -body models for not-yet-studied families
- Trojan families (Rozehnal & Brož 2014), no YE da/dt drift

Future applications (cont.)

- calibration of collisional models based on *young* families
← bias determination is crucial, of course
- both monolith & rubble-pile populations, incl. interactions
- YORP spin-up disruptions (Jacobson et al. 2014)
- combined orbital & collisional models (like LIPAD, Levison et al. 2012)
- 3-dimensional heat diffusion in boulders and meteoroids of various shapes, scaling with D (cf. Breiter et al. 2009)

Future applications (end)

- analyze velocity fields resulting from SPH simulations
- improve scaling of SPH models ($D_{PB} >$ and < 100 km)
- high-speed collisions with weak projectiles (comets)



$D = 100$ km
 $d = 30$ km
 $v = 15$ km/s
 $\phi = 30^\circ$
 $N_{SPH} = 1.56 \cdot 10^5$

Benz & Asphaug (1994)